

An asymptotic theory of the jet flap in three dimensions

By NAOYUKI TOKUDA

Department of Applied Mathematics and Theoretical Physics,
University of Cambridge†

(Received 25 June 1970)

A uniformly valid asymptotic solution has been constructed for three-dimensional jet-flapped wings by the method of matched asymptotic expansions for high aspect ratios. The analysis assumes that the flow is inviscid and incompressible and is formulated on the thin airfoil theory in accordance with the well-established Spence (1961) theory in two dimensions.

A simple method emerges in treating the bound vortices along the jet sheet which forms behind the wing with the aid of the following physical picture. Three distinct flow regions—namely inner, outer and Trefftz—exist in the problem. Close to the wing the flow approximates to that in two dimensions. Therefore, Spence's solution in two dimensions applies. In the outer region a wing shrinks to a line of singularities from which the main disturbances of flow in this region arise. In particular, we find that the shape of the jet sheet, hence the strength of vortices, is now predetermined by the strength of the singularities there. Hence a complete flow field in the outer region can now be determined first by evaluating the flow due to various degrees of singularities along this line and then adding the effect of the jet bound vortices which is now known. Far removed from the wing, the well-known Trefftz region exists in which calculations of aerodynamic forces can be most easily done.

The result has been applied to various wing planforms such as cusped, elliptic and rectangular wings. The present result breaks down for rectangular wings. However, we can apply Stewartson's (1960) solution for lifting-line theory for semi-infinite rectangular wings, because, to this second-order approximation it is established that the jet sheet in the outer region makes no contribution to lift, with the direct contribution of the deflected jet at the exit being cancelled by the reduced circulation in the jet vortices. This result for the rectangular wing gives excellent agreement with the experiments made on a rectangular wing, while the result for elliptic wings underestimates them considerably.

1. Introduction

Because of the current interest in V/STOL applications, high lift devices particularly by means of high-speed jet flow using the abundant air supply of high by-pass engines are receiving considerable interest. The jet flap is one of such better known high lift devices in which the high-speed jet issues in thin

† Present address: Department of Mathematics, University of Southampton

sheets near the trailing edge of the wings providing not only the main propulsive thrust but a high lift force. The original idea of the jet flap is quite old and dates back to the early nineteen-thirties and a detailed historical account on it can be found in an article by Davidson (1956).

In a series of papers Spence (1956, 1958, 1961) has given very extensive analysis of the jet flap in two dimensions. Spence assumes that the jet is concentrated within the thin sheet precluding the mixing of the jet with the ambient fluid. Using the linearized thin airfoil expansion, he can now replace the airfoil and the jet by the vortex sheet placed along the plane of the undisturbed flow whose strength must now be determined by satisfying the flow tangency conditions. The resulting mixed boundary-value problem was solved first by the Fourier expansions (Spence 1956) and then by the Mellin transforms (Spence 1961). Spence's results give remarkable agreement with experimental data even for large jet deflexion angles as high as 60 degrees, indicating that the Spence theory using the thin jet approximation without mixing is well founded.

The importance of the three-dimensional effects in the jet flap application is evident because the jet sheet which forms behind the wing can now sustain the pressure force across it; thus the bound vorticity must now extend not only over the wing but also over the jet sheet. This will act to reduce the effective aspect ratio considerably. See the definition of the effective aspect ratio in § 7 for clarification. Indeed, one of the crucial points in the present three-dimensional analysis is the treatment of the bound vortices along the jet sheet whose shape, hence its vorticity strength, is *a priori* unknown.

A first important extension of the Spence theory to three dimensions was done by Maskell & Spence (1959). They formulated the problem by the lifting surface theory. But the interdependence of the jet vorticity on the flow field makes the analysis almost intractable. Thus being unable to evaluate the downwash field exactly, they used two interpolation formula and were able to express the lift coefficient in terms of the two-dimensional results of Spence (1956) for the special case of uniform downwash in the spanwise direction, namely of elliptic loading. Despite the inexact interpolation methods used, their final results are consistent with the present result. This is because these interpolations are made carefully so that the final results would be always consistent with a clear physical picture presented in their paper. However, some modification is necessary in the asymptotic representation of the result and we discuss their solution further in § 7. Das (1965), on the other hand, resorted to the Multhopp (1955) method in computing the downwash field after the similar formulation by the lifting surface theory. The method then becomes essentially the numerical integration of the downwash field at various positions of pivotal points. The physical interpretation becomes obscured in the process.

The author's attention was drawn to a recent dissertation of Kerney (1967) who applied the method of inner and outer expansions to this problem. Even though his inner and outer solutions seem to match in an analogous manner as in the original work of Van Dyke (1964) for wings without jet flap, there is one serious defect in his analysis. No account is taken by Kerney of the effect of the bound vortices in the outer part of the jet sheet. That this effect cannot be

ignored becomes clear in the light of a physical picture to be presented in §3. Much care is necessary to take this effect into account.

The purpose of this paper is to present an asymptotic theory for the three-dimensional jet-flapped wings which is uniformly valid in the whole flow field except local break-downs either near the wing tip region or the trailing edge region. See §2 and 5 for further discussions on this matter. The problem is formulated in §2 based on the thin airfoil expansion as originally presented by Maskell & Spence (1959) but slightly modified for our purpose of asymptotic theory for high aspect ratios (see Van Dyke (1964) and Kerney (1967)). Using this formulation we present a clear physical picture in §3 which is directly relevant to our analysis. This will not only illuminate the basic structure of the flow field but also greatly facilitates our analysis. An asymptotic solution obtained by the method of matched asymptotic expansions in §4 is consistent with this picture. After deriving the formula for aerodynamic forces on wings in §5, we apply the result of the analysis to flat wings of various wing plan forms such as cusped, elliptic and rectangular wings in §6. For rectangular wings, which are of practical interest, the present solution breaks down. We will show, however, that Stewartson's (1960) elegant solution for the lifting line theory can be applied to the present problem. This result gives remarkable agreement with the experiments of Williams & Alexander (1957) who used a rectangular wing. However, the result for elliptic wings shows some considerable disagreement with these experimental data if the aspect ratio is small and/or C_j is large, namely the effective aspect ratio is small. The reason for this disagreement will be discussed in §7.

2. Formulation

In the analysis, viscosity will be neglected altogether. We should note, however, that by imposing the flow tangency conditions along the wing surface and the jet sheet the present analysis provides a first valid approximation of the inviscid problem in the limit a Reynolds number approaches infinity, provided flow separation is avoided. This inviscid assumption also precludes any jet mixing. Next, following Spence (1956) and Maskell & Spence (1959) we use the thin airfoil theory. This requires that the wing and jet lies close to a plane in which the direction of the undisturbed flow lies so that all the perturbations of the flow caused by them are uniformly small. The validity of this expansion must be interpreted in accordance with the physical situations of the problem. In principle, this expansion is valid at least up to the point of the nearest physical singularity in the problem such as flow separation. Therefore despite small disturbances assumed, τ , the jet deflexion angle, can still be taken as large as $50 \sim 60$ degrees (Spence 1956) but not so for α since the flow separation is more sensitive to α . The problem can now be linearized so that the effect of thickness, incidence and camber may be treated separately. We further assume that the flow is incompressible. Obviously a subsonic flow becomes equivalent to the incompressible flow by the Görtzert rule for small disturbances.

Now consider a cambered wing of zero thickness, whose planform is symmetric

in both span and chordwise directions; see figure 1 for details. We choose the x co-ordinate as the direction of undisturbed uniform flow with a wing inclined from it by a small angle α . The y and z axes are taken in the span-wise direction and in the vertical direction downward, respectively, with the origin at the centre of symmetry. Undisturbed uniform velocity and the wing semi-span length will be chosen as unity without losing any generality. The wing planform will be described by $c(y)/A$ where A is an aspect ratio. From the definition of aspect ratio, we require (see § 6)

$$\int_{-1}^1 c(y) dy = 4.$$

The full governing equation for the velocity potential ϕ in an inviscid incompressible fluid is the Laplace equation

$$\nabla^2 \phi = \phi_{xx} + \phi_{yy} + \phi_{zz} = 0. \quad (2.1)$$

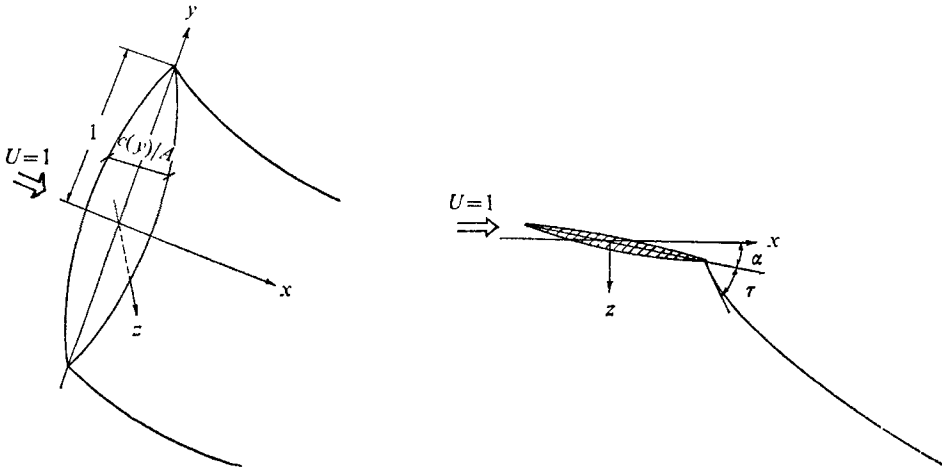


FIGURE 1. Co-ordinate system for jet-flapped wing.

The flow tangency conditions on the basis of the thin airfoil approximations are

on the wing

$$w(x, y, 0) = \epsilon(x, y) + \alpha(y), \quad -c(y)/2A < x < c(y)/2A, \quad (2.2)$$

where $\epsilon(x, y)$ and $\alpha(y)$ denote the camber and the incidence of the wing. u, v, w are the velocity components in x, y , and z direction with $(u, v, w) = (\phi_x, \phi_y, \phi_z)$;

at the trailing edge

$$w(x, y, 0) = \epsilon(x, y) + \alpha(y) + \tau(y) \quad \text{at} \quad x = c(y)/2A, \quad (2.3)$$

τ is the jet deflexion angle at the trailing edge relative to the wing incidence;

on the jet sheet

$$\gamma_j(x, y) = -(cC_j/2A) w_x(x, y, 0). \quad (2.4)$$

Here γ_j is the strength of the bound vorticity within the jet sheet, C_j the jet momentum coefficient defined as $2J/U_\infty^2 \rho c$, where J is the rate of momentum flow of the jet. In deriving this relation, besides the thin jet sheet assumption

of Spence (1956), we further assume that the transverse transport of momentum within the jet, which will exist far downstream due to the rolling up of the vortex sheet, makes little contribution to the total downwash. This assumption may be justified in this problem for the following reasons. As it is well known, the free edge of the vortex sheet curls over under the influence of the induced velocity field of the vortex sheet, thus initiating the rolling-up process. In this problem, however, because of the large momentum in the jet sheet, the trailing vortex sheet becomes considerably stiffened, thus delaying the rolling-up process further downstream. In this sense, the jet sheet behaves more like a solid plane sheet rather than a free vortex sheet. Far enough downstream, the rolling-up of the sheet still takes place. It is noted, however, that even then the total jet vorticity strength is not likely to change much because the additional contribution from the transverse jet momentum to the vorticity strength tends to be compensated by the reduced contribution of the lateral jet momentum as the rolling-up implies the reduced downwash towards the edges. Another important reason which justifies this assumption is that, in practice, the jet sheet which originally carries a large momentum dissipates itself and loses much of its momentum by the entrainment far downstream. That is, at a sufficiently downstream point where the rolling-up takes place, the jet vorticity strength is likely to be very small; the effect of the rolling-up on the downwash should, therefore, be very small. Indeed the excellent agreement of our analytical model with the experiment supports our argument above. Then (2.4) follows readily by noting that this bound vorticity is introduced to replace the pressure discontinuity across the jet sheet. This pressure discontinuity can be evaluated as the centrifugal force of the thin jet due to the sheet curvature. See Maskell & Spence (1959) for the details of the derivation. The discontinuity of the flow tangency at the trailing edge introduced by the jet sheet condition of (2.3) gives rise to a logarithmic singularity in the bound vorticity (Spence 1956). Therefore, the velocity on the upper side of the jet sheet becomes unbounded while that on the lower side must be stagnant. The relation (2.4) which does not take this stagnation condition into account apparently breaks down. However, the more exact treatment of Ackerberg (1968) has shown that this singular region is concentrated in a very thin boundary-layer type region for small τ and the integrated effect such as lift force is little affected by this local breakdown of the solution.

Far from the wing, the flow must approach the uniform flow.

Far from the wing

$$\phi \sim x \quad \text{for} \quad x^2 + y^2 + z^2 \rightarrow \infty \quad \text{but not} \quad z = 0. \quad (2.5)$$

We will now examine the problem within the framework of the above formulation and derive some important physical pictures.

3. Physical background

A standard technique to solve equations (2.1) to (2.5) for a finite aspect ratio A is to replace the wing and the jet sheet by such a distribution of the bound vorticity that the required boundary conditions are satisfied when its effect is integrated

over the whole vorticity field by the Biot–Savart law. Any change in the bound vorticity distribution must be accompanied by a system of horse-shoe trailing vortices. The resulting singular double integral equations with mixed boundary conditions seem intractable to any rigorous analysis with little possibility for further simplification. Some substantial approximations such as interpolations (Maskell & Spence 1959) or a resort to the numerical approach (Das 1965) are necessary to make progress from this lifting surface type approach.

A remarkably simple approach emerges, however, if we examine the equations (2.1) to (2.5) carefully for large aspect ratios. This can be best demonstrated with a particular reference to figure 2. This following argument is important to the correct understanding of the problem.

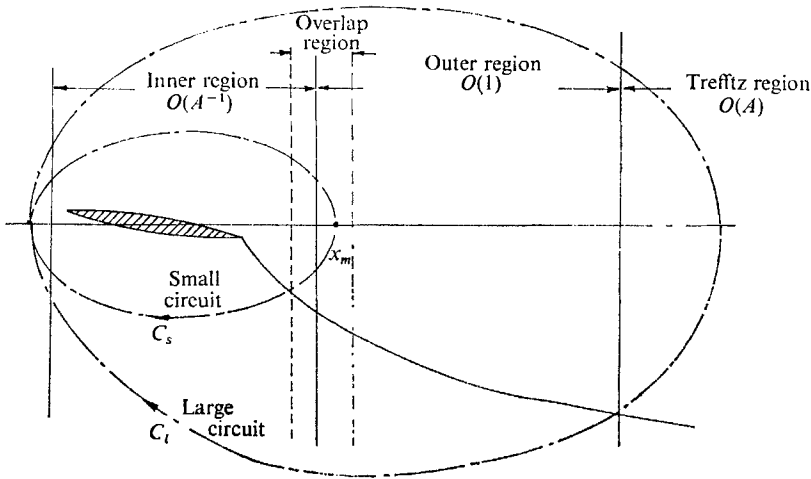


FIGURE 2. Basic-flow structure.

We see that three distinct flow regions exist in this problem.

Close to the wing whose chord and span length are of $O(1/A)$ and $O(1)$ respectively the flow is dominated by the bound vorticity of the wing including the portion of jet sheet near the wing. This is so because to an observer in this domain the wing seems to extend to infinity.† In this inner region, the flow approximates to that of two dimensions. This can be easily confirmed by choosing the inner variables

$$X = Ax, \quad Y = y, \quad Z = Az \quad \text{with} \quad A \rightarrow \infty, \quad (3.1)$$

since then the Laplacian operator reduces to the two-dimensional one.

Now if we are away from the wing at a distance of $O(1)$, to an observer in this domain, the length scale of wing chord vanishes with the wing shrinking to a line. This line becomes the main source for disturbances to the otherwise uniform flow in this domain. This situation corresponds exactly to the more familiar Oseen region in viscous flows. See Lagerstrom (1964, p. 98) for the similar

† This would obviously not be true near the tip of the wing. However, this local breakdown of the analysis is not serious for most of the well-shaped wing forms. This defect becomes serious for rectangular wings for example, see §6, for the details.

physical interpretation. Now in the presence of the jet sheet, this non-uniformity of the flow means that, besides a system of trailing vortices originating from the inner domain, the bound vorticity exists in this domain. The reason is now evident. Because the jet sheet must be the streamline of the flow, any deviation of the flow from the uniform flow implies the existence of curvature in the jet sheet and, hence, the pressure discontinuity across it due to the non-zero jet momentum. From our observation above of the wing as a singular line, one of the most important results in this work emerges. That is, the shape of the jet sheet and hence the strength of the bound vorticity in this outer domain is actually pre-determined by the strength of singularities along this line. To see this mathematically, it is sufficient to note that the jet vorticity given in (2.4) is of higher order than the velocity field itself in the outer domain while in terms of the inner variables, they become of the same order. We then see that in the outer region the flow determines the jet shape but in the inner region they are completely interdependent. See equations (4.2) and (4.10) to follow for details.

Finally we should note that if $x = O(A)$, far removed from the wing, the Laplacian operator again reduces to that of two dimensions but this time in the (y, z) plane which is normal to the main-stream direction. The importance of this plane is recognized by Trefftz (1921) since the aerodynamic forces on the wing such as drag and lift can be calculated by knowing the flow properties in this plane. The trace of the vortex sheet in the slit in this plane must now account for all the bound vorticity distribution in the streamwise direction including the inner and outer regions. We will see then that in the analysis, we need the circulation in two different circuits as shown in figure 2, one in a smaller circuit C_s extending up to the overlap domain and the other in a large circuit C_l spanning this Trefftz plane enclosing the whole inner and outer regions. We need the former to represent the strength of singularities in the inner region and the latter to compute the aerodynamic forces.

The asymptotic solution we obtain in § 4 by the method of matched expansions is consistent with this physical picture; because Kerney (1967) has not taken into account the existence of the jet bound vorticity in the outer region which obviously exists, as this argument shows, his solution is incomplete despite the fact that his inner and outer solutions seem to match.

4. Solution

4.1. Outer limit

We will seek the solution as $A \rightarrow \infty$ with x, y, z fixed. Because the wing shrinks to a line, the inner boundary conditions applied on the wing equations (2.2) and (2.3) cannot be enforced. Hence the governing equations are

$$\phi_{xx} + \phi_{yy} + \phi_{zz} = 0, \quad (4.1)$$

$$\gamma_j = -(cC_j/2A) w_x(x, y, 0) \quad (x > x_m), \quad (4.2)$$

$$\phi \sim x \quad \text{as} \quad x^2 + y^2 + z^2 \rightarrow \infty \quad (z \neq 0). \quad (4.3)$$

Here x_m is a point in the overlap domain where the matching is carried out, as sketched in figure 2. The missing inner boundary conditions on the wing must

be replaced by the matching requirement as given in §4.2 below. We see that the potential ϕ and corresponding velocity components can be expanded as

$$\left. \begin{aligned} \phi(x, y, z, 1/A) &= \phi_1(x, y, z) + (1/A)\phi_2(x, y, z) + (1/A^2)\phi_3(x, y, z), \\ w(x, y, z, 1/A) &= w_1 + (1/A)w_2 + (1/A^2)w_3 + \dots \end{aligned} \right\} \quad (4.4)$$

To the first approximation, there arise no disturbances from the wing.

$$\phi_1 = x \quad \text{hence} \quad w_1 = 0. \quad (4.5)$$

This means that the first-order inner solution must satisfy the uniform outer flow condition exactly. Before examining the inner expansions, we will clarify the simplified matching procedure used throughout this analysis.

4.2. Matching procedure

The success of the method of the inner and outer expansions, of course depends on the existence of the overlap domain in the intermediate region. This is clearly demonstrated by Van Dyke (1964) for wings without jet flap. The physical picture presented in §3 suggests that this should also be true with the presence of the jet flap. Now the matching must be carried out for any sector of the overlap domain. For the simplification of the analysis we use a special sector for this matching. Namely,

- the inner representation of the outer solution with z/x fixed (say C)
- = the outer representation of the inner solution with $Z/X (= C)$. (4.6)

This point seems to be first brought out by Ashley & Landahl (1966, p. 141). We choose $C = 0$ rather than ∞ which is chosen by Ashley & Landahl. This now allows us to match the outer downwash field w and the inner downwash W on the plane $z = 0$ in the overlap domain. The matching of the downwash field at $Z = 0$ has also been used by Kerney (1967).

4.3. Inner limit

In the inner limit, we seek the solution as $A \rightarrow \infty$ with inner variables X, Y, Z fixed. We also must stretch the potential ϕ if the inner boundary conditions are to be satisfied. Hence,

$$\phi = A^{-1}\Phi(X, Y, Z, 1/A) \quad \text{as} \quad X, Y, Z \quad \text{fixed as} \quad A \rightarrow \infty,$$

where from (3.1), $X = Ax, Y = y, Z = Az$. Now the governing equations are

$$\Phi_{XX} + \Phi_{ZZ} = -\Phi_{YY}/A^2, \quad (4.7)$$

$$W(X, Y, 0) = \epsilon(X, Y) + \alpha(Y), \quad -\frac{1}{2}c(Y) < X < \frac{1}{2}c(Y), \quad (4.8)$$

$$W(X, Y, 0) = \epsilon(X, Y) + \tau(Y), \quad X = \frac{1}{2}c(Y), \quad (4.9)$$

$$\gamma_j(X, Y) = -\frac{1}{2}c_j W_X(X, Y, 0), \quad X > \frac{1}{2}c(Y). \quad (4.10)$$

The potential Φ , therefore the corresponding velocity components (U, V, W), can be shown to have the following expression:

$$\left. \begin{aligned} \Phi(X, Y, Z, 1/A) &= \Phi_1(X, Y, Z) + \Phi_2(X, Y, Z)/A + O(\ln A/A^2), \\ W(X, Y, Z, 1/A) &= W_1(X, Y, Z) + W_2(X, Y, Z)/A + O(\ln A/A^2), \\ \dots\dots\dots \end{aligned} \right\} \quad (4.11)$$

We will see that the logarithmic term must intervene at the third approximation of the inner expansion for the jet flap case just as in Van Dyke's (1964) analysis. See (4.41) for further details.

Substituting (4.11) into (4.7) to (4.10), we easily find that Φ_1 must satisfy the two-dimensional problem at each section Y as studied by Spence (1956). Except for Hough's (1959) work which was a study of the jet flap with parabolic camber distribution, all the existing two-dimensional solutions assume zero camber or $\epsilon = 0$. In the analysis to follow, we also assume that $\epsilon(X, Y) = 0$, but the same analysis follows even if $\epsilon \neq 0$.

It is well known that the complex velocity of a thin lifting airfoil in two dimensions can be expressed in terms of the local strength of vortices placed on the axis by the Cauchy-Riemann relation. Now the first-order inner solution which matches (4.5) is

$$U_1 - iW_1 = 1 + \frac{1}{2\pi i} \int_{-\frac{1}{2}\epsilon(Y)}^{\infty} \frac{\Gamma_1(X', Y)}{X + iZ - X'} dX'. \tag{4.12}$$

Note that (4.12) satisfies the uniform flow condition as $Z \rightarrow \infty$. Γ_1 has been determined by Spence superimposing the effect of α and τ as

$$\Gamma_1(X, Y) = \tau f_1(X, C_j) + \alpha f_2(X, C_j).$$

In terms of lift coefficient $C_L^{(2)}$ in two dimensions

$$C_L^{(2)} = \frac{2}{c} \int_{-\frac{1}{2}\epsilon(Y)}^{\infty} \Gamma_1(X, Y) dx = \alpha \frac{\partial C_L^{(2)}}{\partial \alpha} + \tau \frac{\partial C_L^{(2)}}{\partial \tau}. \tag{4.13}$$

Spence (1961) gives $\partial C_L^{(2)}/\partial \alpha$ and $\partial C_L^{(2)}/\partial \tau$ as

$$\frac{\partial C_L^{(2)}}{\partial \alpha} = 2\pi \left[1 - \frac{C_j}{4\pi} \left(1 + \frac{C_j}{4\pi} \right) \left(\log \frac{C_j}{4\beta} - 1 \right) + O(C_j^2) \right], \tag{4.14}$$

$$\frac{\partial C_L^{(2)}}{\partial \tau} = 2(\pi C_j)^{\frac{1}{2}} \left[1 - \frac{C_j}{8\pi} \log \frac{C_j}{4\beta} - \frac{C_j^2}{128\pi^2} \left\{ \left(\log \frac{C_j}{4\beta} \right)^2 + 4 \log \frac{C_j}{4\beta} - 4 \right\} + O(C_j^2) \right], \tag{4.15}$$

where $\beta = 4e^\gamma$, γ being Euler's constant 0.5772....

We can formally expand the imaginary part of (4.12) with $Z = 0$ to obtain

$$W_1 \sim \frac{\gamma_1}{2\pi X} + \frac{m_1}{2\pi X^2} + \frac{n_1}{2\pi X^3} + \dots, \tag{4.16}$$

where
$$\left. \begin{aligned} \gamma_1 &= \int_{-\frac{1}{2}\epsilon}^{\infty} \Gamma_1 dX = \frac{1}{2}cC_L^{(2)}, \quad \text{with } C_L^{(2)} = \frac{\partial C_L^{(2)}}{\partial \alpha} \alpha + \frac{\partial C_L^{(2)}}{\partial \tau} \tau, \\ m_1 &= \int_{-\frac{1}{2}\epsilon}^{\infty} X' \Gamma_1 dX', \quad n_1 = \int_{-\frac{1}{2}\epsilon}^{\infty} X'^2 \Gamma_1 dX', \dots \end{aligned} \right\} \tag{4.17}$$

γ_1 corresponds to the circulation, while m_1 expresses the pitching moment around the leading edge due to the distributed vortices and the following terms denote successively higher-order moments.

4.4. Second approximation

Outer solution. As evident from Van Dyke's analysis, a solution for the second-order outer expansion ϕ_2 which matches the first term of W_1 in (4.16), can be constructed by placing a line vortex along $x = 0$ to which the wing shrinks in

this outer limit. This strength of circulation must be defined in a smaller circuit C_s of figure 2 which encloses the wing and the whole inner region. This circulation has also the following expansion:

$$l(y, 1/A) = l_2(y)/A + l_3(y)/A^2 + \dots \tag{4.18}$$

To complete the outer flow field however, one must add the effect of the jet bound vorticity γ_j from this order. For disturbances now arise in this domain in otherwise uniform flow by the presence of the wing and jet. Since ϕ_2 is $O(1/A)$, (4.2) shows that γ_j is $O(1/A^2)$ and is therefore of higher-order effect. However, we must recognize that γ_j unlike the line vortex l is distributed uniformly over the whole outer field. Therefore the accumulated effect of γ_j may possibly have the effect of $O(1/A)$. Such a situation arises in linear supersonic flow whose paradox was successfully resolved by Whitham (1952). However, in the present problem, because $\gamma_j \propto w_x$ or γ_j is the exact differential of the velocity with respect to x , the integrated effect still remains of $O(1/A^2)$. So this effect will not appear until the next approximations. Hence, w_2 at $Z = 0$ is given as

$$w_2 = -\frac{1}{4\pi} \frac{\partial}{\partial y} \int_{-1}^1 \frac{l_2}{y-y_1} \left\{ 1 + \frac{[x^2 + (y-y_1)^2]^{\frac{1}{2}}}{x} \right\} dy_1. \tag{4.19}$$

Expanding by the inner variables

$$w_2 \sim \frac{l_2}{2\pi x} + \alpha_{i_2} \quad (x \rightarrow 0). \tag{4.20}$$

For large x

$$w_{2\infty} \sim 2\alpha_{i_2} \quad (x \rightarrow \infty), \tag{4.21}$$

where

$$\alpha_{i_2} = -\frac{1}{4\pi} \frac{\partial}{\partial y} \int_{-1}^1 \frac{l_2}{y-y_1} dy_1. \tag{4.22}$$

Here α_{i_2} is the induced incidence. By matching,

$$l_2 = \gamma_1 = \frac{1}{2} c C_L^{(2)}. \tag{4.23}$$

Inner solution. From (4.20), we confirm that Φ_2 of (4.11) is the correct inner term to this order. Φ_2 still satisfies the Laplace equation in two dimensions. Furthermore, the boundary conditions introduced by the induced incidence α_{i_2} of (4.20) suggest that Φ_2 is simply the result of reducing the incidence angle α by α_{i_2} . Hence the solution for Φ_2 follows immediately from Spence's solution by putting $\alpha = -\alpha_{i_2}$, $\tau = 0$ in (4.13) (see also Kerney 1967).

$$U_2 - iW_2 = \frac{1}{2\pi i} \int_{-\frac{1}{2}c(Y)}^{\infty} \frac{\Gamma_2(X', Y)}{X + iZ - X'} dX'.$$

W_2 at $Z = 0$ can be expanded as

$$W_2 \sim \frac{\gamma_2}{2\pi X} + \frac{m_2}{2\pi X^2}, \tag{4.24}$$

$$\gamma_2 = \int_{-\frac{1}{2}c}^{\infty} \Gamma_2 dX', \quad m_2 = \int_{-\frac{1}{2}c}^{\infty} X' \Gamma_2 dX', \tag{4.25}$$

where

$$\int_{-\frac{1}{2}c}^{\infty} \Gamma_2 dX' = \frac{1}{2} C_L^{(2)} = -\frac{1}{2} c \alpha_{i_2} \partial C_L^{(2)} / \partial \alpha.$$

Hence to this order, the outer expansion of the inner expansion is

$$W \sim W_1 + W_2/A \sim \frac{\gamma_1}{2\pi Ax} + \frac{\alpha_{i_2}}{A} + \frac{1}{A^2} \left\{ \frac{m_1}{2\pi x^2} + \frac{\gamma_2}{2\pi x} \right\} + O(1/A^3). \tag{4.26}$$

4.5. Third approximation

Outer solution. The outer flow to this order becomes more complex because besides the line vortex, we further need the higher-order vortex distribution (called divortex by Van Dyke 1964) to match to the term m_1/x^2 of (4.26) and most important in this problem, jet vortex sheet starts to have effect. We write

$$w_3 = w_{3l} + w_{3d} + w_{3j}. \tag{4.27}$$

Subscripts l, d and j refer to the flow due to the line vortex, divortex and jet sheet respectively. They will be determined in the following.

w_{3l} : flow due to line vortex. Equation (4.26) shows that l_3 is $O(A^{-2})$ as given by (4.18). Therefore w_{3l} can be expressed in the same form as w_2 of (4.19),

$$w_{3l} = -\frac{1}{4\pi} \frac{\partial}{\partial y} \int_{-1}^1 \frac{l_3}{y-y_1} \left[1 + \frac{[x^2 + (y-y_1)^2]^{\frac{3}{2}}}{x} \right] dy_1. \tag{4.28}$$

Now l_3 must be the strength of the circulation in the smaller circuit C_s which intersects the x axis at x_m . Besides γ_2 of (4.26), both the residue of γ_1 beyond x_m and the induced incidence α_{i_2} turn out to have the effect of $O(A^{-2})$. Taking these into account, l_3 can be shown to be

$$l_3 = \gamma_2 - \frac{cC_j}{4\pi x_m} \gamma_1 - \frac{cC_j}{2} \alpha_{i_2}. \tag{4.29}$$

This result follows from the expansion of W in (4.26). Compare this with that given in (4.38).

Now we define the induced incidence in this order by $\alpha_{i_{30}}, \alpha_{i_{31}}$ and $\alpha_{i_{32}}$.

$$\left. \begin{aligned} \alpha_{i_{30}} &= -\frac{1}{4\pi} \frac{\partial}{\partial y} \int_{-1}^1 \frac{\gamma_2}{y-y_1} dy_1, \\ \alpha_{i_{31}} &= -\frac{1}{4\pi} \frac{\partial}{\partial y} \int_{-1}^1 \frac{cC_j \gamma_1}{y-y_1} dy_1, \\ \alpha_{i_{32}} &= -\frac{1}{4\pi} \frac{\partial}{\partial y} \int_{-1}^1 \frac{cC_j \alpha_{i_2}}{y-y_1} dy_1. \end{aligned} \right\} \tag{4.30}$$

It turns out that $\alpha_{i_{31}}$ cancels out and does not appear in the final result. Then for $x \rightarrow 0$

$$w_{3l} \sim \left(\frac{\gamma_2}{2\pi x} - \frac{cC_j \gamma_1}{8\pi^2 x x_m} - \frac{cC_j \alpha_{i_2}}{4\pi x} \right) + \left(\alpha_{i_{30}} - \frac{\alpha_{i_{31}}}{4\pi x_m} - \frac{\alpha_{i_{32}}}{2} \right) + O(x). \tag{4.31}$$

For $x \rightarrow \infty$

$$w_{3l} \sim \left(2\alpha_{i_{30}} - \frac{\alpha_{i_{31}}}{2\pi x_m} - \alpha_{i_{32}} \right) + O\left(\frac{1}{x}\right). \tag{4.32}$$

w_{3d} : flow due to divortex. Successively higher-order singularities are necessary in the outer expansion to match to the terms corresponding to the higher-order moment of the distributed vorticity in the inner expansion such as $m_1/x^2, n_1/x^3, \dots$

of (4.16). For the first moment which is physically the pitching moment, Van Dyke (1964) has shown that the potential of a divortex distribution which is the x -derivative of that for the line vortex must be used. The divortex strength δ can be expanded as

$$\delta = \frac{\delta_3}{A^2} + \frac{\delta_4}{A^3} + \dots$$

w_{3d} can now be given at $z = 0$ as (Van Dyke 1964)

$$w_{3d} = \frac{1}{4\pi^2} x^2 \frac{\partial}{\partial y} \int_{-1}^1 \delta_3 \frac{y - y_1}{[x^2 + (y - y_1)^2]^{\frac{3}{2}}} dy_1. \tag{4.33}$$

The strength of the divortex δ_3 can be determined by matching

$$\delta_3 = \pi m_1. \tag{4.34}$$

w_{3j} : flow due to jet vorticity. The downwash field w_{3j} due to the jet sheet vortices can only be expressed by using the full lifting surface expression,

$$w_{3j} = -\frac{1}{4\pi} \frac{\partial}{\partial y} \int_{-1}^1 \int_{x_m}^{\infty} \frac{\gamma_j}{y - y_1} \left[1 + \frac{[(x - x_1)^2 + (y - y_1)^2]^{\frac{1}{2}}}{x - x_1} \right] dx_1 dy_1. \tag{4.35}$$

Now the jet vorticity γ_j has the following expansion:

$$\gamma_j = \frac{\gamma_{j3}}{A^2} + \frac{\gamma_{j4}}{A^3} + \dots$$

From the boundary condition (4.2) and the physical arguments γ_{j3} is now pre-determined by w_2

$$\gamma_{j3} = -\frac{1}{2} c C_j w_{2x} = \frac{c C_j}{8\pi} \frac{\partial^2}{\partial x \partial y} \int_{-1}^1 \frac{\gamma_1}{y - y_1} \left[1 + \frac{[x^2 + (y - y_1)^2]^{\frac{1}{2}}}{x} \right] dy_1. \tag{4.36}$$

Although w_{3j} cannot be readily expressed in an explicit form, we can find a few terms of the asymptotic expansion as $x \rightarrow 0$ and $x \rightarrow \infty$. Write $w_{3j} = w_{3j_1} + w_{3j_2}$,

$$\begin{aligned} w_{3j_1} &= -\frac{1}{4\pi} \frac{\partial}{\partial y} \int_{-1}^1 \int_{x_m}^{\infty} \frac{\gamma_{j3}}{x_m y - y_1} dx_1 dy_1 \\ w_{3j_2} &= -\frac{1}{4\pi} \frac{\partial}{\partial y} \int_{-1}^1 \int_{x_m}^{\infty} \frac{\gamma_{j3}}{x_m y - y_1} \frac{[(x - x_1)^2 + (y - y_1)^2]^{\frac{1}{2}}}{x - x_1} dx_1 dy_1. \end{aligned} \tag{4.37}$$

Note
$$\int_{x_m}^{\infty} \gamma_{j3} dx_1 = -\frac{1}{2} c C_j w_2 \Big|_{x_m}^{\infty} = \frac{\gamma_1}{4\pi x_m} - \frac{1}{2} c C_j \alpha_{i_2}. \tag{4.38}$$

From (4.38)
$$w_{3j_1} = \frac{\alpha_{i_{31}}}{4\pi x_m} - \frac{\alpha_{i_{32}}}{2}. \tag{4.39}$$

For $x \rightarrow 0$ with $x_m \ll x$, w_{3j_2} can be approximated.

$$w_{3j_2} = -\frac{1}{4\pi} \frac{\partial}{\partial y} \int_{-1}^1 \int_{x_m}^{\infty} \frac{\gamma_{j3}(x_1, y_1)}{x} \text{sign}(y - y_1) dx_1 dy_1. \tag{4.40}$$

This is so because the dominant term of the integral comes from the singularity at $x_1 = x_m$. We note that the singularity of the integral at $x_1 = x$ is anti-symmetric

near $x_1 = x$ so that the contribution from this region may be obtained by the Cauchy principal value of the integral. A rough check suggests this is $O(\ln x_m/x^2)$. Because $w_2 \sim (\gamma_1/2\pi x_m) + \alpha_{i_1}$ as $x_m \rightarrow 0$ the contribution of the integral from the immediate neighbourhood of $x = x_m$ is $(cC_j\gamma_1/8\pi^2 x_m) + (cC_j/4\pi x)\alpha_{i_1}$.

Hence
$$w_{3j_2} \sim \frac{cC_j\gamma_1}{8\pi^2 x_m} + \frac{cC_j\alpha_{i_2}}{4\pi x} + O\left(\frac{\ln x_m}{x^2}\right) \quad \text{as } x \rightarrow 0. \tag{4.41}$$

There should arise a constant term $\alpha_{i_{3j}}$ in (4.41) corresponding to the induced incidence due to this jet sheet. This can only be evaluated if we can evaluate (4.37) more exactly and remains undetermined.

For $x \rightarrow \infty$, the leading term of w_{3j_2} is equal to w_{3j_1}

$$w_{3j_2} = \frac{\alpha_{i_{31}}}{4\pi x_m} - \frac{\alpha_{i_{32}}}{2}. \tag{4.42}$$

Hence w_3 will behave as follows. For $x \rightarrow 0$

$$w_3 \sim \left[\frac{m_1}{2\pi x_2} + \frac{\gamma_2}{2\pi x} + (\alpha_{i_{30}} - \alpha_{i_{32}} + \alpha_{i_{3j}}) + O(x) \right] + O(\ln A/A^2). \tag{4.43}$$

We see that $O(\ln A/A^2)$ term must precede the $O(1/A^2)$ term in the next inner expansion in agreement with Van Dyke's (1964) analysis.

Now if $x \rightarrow \infty$

$$w_{3\infty} \sim 2[\alpha_{i_{30}} - \alpha_{i_{32}}] + O(1/x). \tag{4.44}$$

Although the downwash $w_{3\infty}$ at $x = \infty$ is known exactly, induced incidence at the wing as $x \rightarrow 0$ is not known due to $\alpha_{i_{3j}}$. Because the jet bound vorticity is distributed over the whole downstream region of the wing, unlike conventional wing theory which requires $\alpha_{i_\infty} = 2\alpha_i$, $\alpha_{i_{3j}}$ does not have to vanish. We see that the induced incidence to this order now arises not only from the circulation in the inner domain $\alpha_{i_{30}}$, but also from the jet sheet bound vorticity, $\alpha_{i_{32}}$ and $\alpha_{i_{3j}}$. With this induced incidence providing new boundary conditions, the third term inner solution can be formally formulated. As in Van Dyke, one must add a logarithmic term in the expansion. However, with the presence of the jet flap, a solution for the two-dimensional Poisson equations seem too complicated to obtain a useful result. We will show in the following that the solution obtained so far provides the two terms of the asymptotic series in lift and drag which already provides acceptable results.

5. Aerodynamic forces

Aerodynamic forces acting on wings such as lift and drag forces can be most easily evaluated by considering the large control volume along a large circuit C_i of figure 2 which intersects with the Trefftz plane. In our problem we must add the direct contribution to the lift and drag forces of the jet thrust at the exit, because the jet remains deflected. Maskell & Spence (1959) and Kerney (1967) have shown then that the coefficient for lift and the induced drag can be expressed in terms of the flow quantities in the Trefftz plane. Kerney particularly

gives a detailed derivation on this issue. The results for the lift coefficient C_L and induced drag coefficient C_{Di} are

$$C_L = \frac{A}{2} \int_{-\infty}^{\infty} \int_{-\infty}^{\infty} w_{\infty}(y, z) dz dy + \frac{1}{4} \int_{-1}^1 cC_j w_{\infty}(y, 0) dy,$$

$$C_{Di} = \frac{A}{4} \int_{-\infty}^{\infty} \int_{-\infty}^{\infty} (v_{\infty}^2 + w_{\infty}^2) dz dy + \frac{1}{8} \int_{-1}^1 cC_j w_{\infty}^2(y, 0) dy.$$

Here w_{∞} and v_{∞} are the velocity components in the Trefftz plane, and the integration is required over the whole Trefftz plane. Noting that

$$\int_{-\infty}^{\infty} w_{\infty}(y, z) dz = L,$$

L being the circulation in a large circuit C_l , C_L and C_{Di} can be expressed in terms of $w_{\infty}(y, 0)$ and L (Kerney 1967),

$$C_L = \frac{A}{2} \int_{-1}^1 L(y) dy + \frac{1}{4} \int_{-1}^1 cC_j w_{\infty}(y, 0) dy, \tag{5.1}$$

$$C_{Di} = \frac{A}{2} \int_{-1}^1 w_{\infty} L dy + \frac{1}{8} \int_{-1}^1 cC_j w_{\infty}^2 dy. \tag{5.2}$$

The circulation L in a large circuit C_l will now enclose both inner and outer regions. Therefore L must include both the line vorticity l and the bound vorticity in the jet γ_j in the outer region

$$L = l + \int_{x_m}^{\infty} \gamma_j dx = \frac{l_2}{A} + \frac{l_3}{A^2} - \frac{cC_j}{2A^2} w_2 \Big|_{x_m}^{\infty} + O\left(\frac{\ln A}{A^3}\right).$$

Using (4.23) and (4.29) and (4.20) and (4.21),

$$L = \frac{\gamma_1}{A} + \frac{1}{A^2} (\gamma_2 - cC_j \alpha_{i_2}) + O\left(\frac{\ln A}{A^3}\right), \tag{5.3}$$

$\gamma_1, \gamma_2, \alpha_{i_2}$ are all found in § 4.

The downwash velocity in the Trefftz plane w_{∞} is

$$w_{\infty} = \frac{2\alpha_{i_2}}{A} + \frac{2}{A^2} (\alpha_{i_{30}} - \alpha_{i_{32}}) + O\left(\frac{\ln A}{A^3}\right), \tag{5.4}$$

where $\alpha_{i_2}, \alpha_{i_{30}}$ and $\alpha_{i_{32}}$ are given in (4.22) and (4.30).

Substituting L and w_{∞} one finally obtains

$$C_L = \frac{1}{2} \int_{-1}^1 \gamma_1 dy + \frac{1}{2A} \int_{-1}^1 \gamma_2 dy + O\left(\frac{1}{A^2}\right), \tag{5.5}$$

$$C_{Di} = \frac{1}{2A} \int_{-1}^1 \alpha_{i_2} \gamma_1 dy + \frac{1}{2A^2} \int_{-1}^1 \{\gamma_1 (\alpha_{i_{30}} - \alpha_{i_{32}}) + \gamma_2 \alpha_{i_2}\} dy + O\left(\frac{1}{A^2}\right). \tag{5.6}$$

$\gamma_1, \gamma_2, \alpha_{i_2}, \alpha_{i_{30}}, \alpha_{i_{32}}$ have already been obtained in (4.17), (4.25), (4.22) and (4.30) respectively.

We should particularly note here that, to this order of approximation, the direct positive lift contribution from the deflected jet sheet at the exit is cancelled by the reduced jet bound vorticity in the outer flow. Hence the correct lift coefficient is given by merely integrating the two-dimensional inner solution in

a spanwise direction without adding the extra jet exit momentum as given by (5.5). This can be easily checked since the strength of the jet bound vorticity is an exact differential of the downwash field. The decrease of the circulation in the jet sheet from that of the two-dimensional value is $\frac{1}{2}cC_j w_\infty$ but this is exactly the added amount of lift force due to the deflected jet. Also we note that the induced incidence arising from the jet vorticity now affects the drag term.

6. Application to a family of planforms

Following Van Dyke (1964), we apply the result to a family of wing planforms. Each of the following wings has an aspect ratio A from our definition:

$$\left. \begin{aligned}
 \text{wing } a, \text{ cusped wing} & \quad c(y) = \frac{32}{3\pi} (1-y^2)^{\frac{3}{2}}, \\
 \text{wing } b, \text{ lenticular (parabolic) wing} & \quad c(y) = \frac{3}{2}(1-y^2), \\
 \text{wing } c, \text{ elliptic wing} & \quad c(y) = \frac{8}{\pi} (1-y^2)^{\frac{1}{2}}, \\
 \text{wing } d, \text{ rectangular wing} & \quad c(y) = 2H(1-y^2).
 \end{aligned} \right\} \quad (6.1)$$

Here H above denotes the Heaviside step function.

Given the wing planform $c(y)$ and further assuming that C_j , α and τ are constant along the spanwise direction, one can now integrate (5.5) and (5.6) for each wing planform. Some of the contour integration required in the reduction of this integral will be described in the appendix and the results only will be given below. Van Dyke (1964) clearly demonstrated that, for these wing problems, a fractional form always improves the approximation considerably. So the final results are given in this fractional form.

Wing a: cusped wing

$$\left. \begin{aligned}
 \frac{C_L}{C_L^{(2)}} &= 1 / \left[1 + \frac{8}{3\pi A} \frac{\partial C_L^{(2)}}{\partial \alpha} \right], \\
 \frac{C_{D_i}}{(C_L^{(2)})^2} &= \left(\frac{8}{3\pi A} \right)^2 / \left[\frac{8}{3\pi A} + \frac{1}{A^2 \pi^2} \left(13C_j + \frac{140}{2\pi} \frac{\partial C_L^{(2)}}{\partial \alpha} \right) \right].
 \end{aligned} \right\} \quad (6.2)$$

Wing b: lenticular wing

$$\left. \begin{aligned}
 \frac{C_L}{C_L^{(2)}} &= 1 / \left[1 + \frac{9}{8\pi A} \frac{\partial C_L^{(2)}}{\partial \alpha} \right], \\
 \frac{C_{D_i}}{(C_L^{(2)})^2} &= \left(\frac{9}{8\pi A} \right)^2 / \left[\frac{9}{8\pi A} + \frac{1}{A^2 \pi^2} \left(\left(\frac{3}{40} + \frac{9}{4\pi^2} \right) C_j + \left(\frac{3}{40} + \frac{9}{8\pi^2} \right) \frac{\partial C_L^{(2)}}{\partial \alpha} \right) \right].
 \end{aligned} \right\} \quad (6.3)$$

Wing c: elliptic wing

$$\left. \begin{aligned}
 \frac{C_L}{C_L^{(2)}} &= 1 / \left[1 + \frac{1}{\pi A} \frac{\partial C_L^{(2)}}{\partial \alpha} \right], \\
 \frac{C_{D_i}}{(C_L^{(2)})^2} &= \left(\frac{1}{\pi A} \right)^2 / \left[\frac{1}{\pi A} + \frac{1}{\pi^2 A^2} \left(2C_j + 2 \frac{\partial C_L^{(2)}}{\partial \alpha} \right) \right].
 \end{aligned} \right\} \quad (6.4)$$

For an elliptic wing, C_{D_i} may be rewritten as

$$C_{D_i} = \frac{1}{\pi A} \left\{ \frac{C_L^{(2)}}{1 + \frac{1}{\pi A} \frac{\partial C_L^{(2)}}{\partial \alpha}} \right\}^2 \frac{1}{1 + \frac{2C_j}{\pi A}}.$$

Hence
$$C_L = \frac{C_{D_i}}{\pi A + 2C_j}. \quad (6.5)$$

This relation must hold exactly for wings of elliptic loading with the jet flap as first pointed out by Maskell & Spence (1959).

A similar integration of C_L and C_{D_i} for rectangular wings leads to meaningless divergent results. This is physically expected (see §3). This is because near the tip of the wing, the induced load must become of the same order of the original load given by the two-dimensional analysis and the present perturbation scheme breaks down. It is true that a similar breakdown occurs for wing b and c locally near the tip of the distance $O(e^{-A})$ and $O(A^{-2})$ respectively. However, since the original load itself vanishes in proportion to the chord length, C_L and C_{D_i} can still be integrated. See Van Dyke (1964) for detailed discussions. For wings without jet flap, this defect has been corrected by Stewartson (1960) by isolating the tip and solving the problem of lifting semi-infinite rectangular wings. Stewartson's result can be applied to the present problem with the jet flap at least to $O(A^{-1})$, because, as we have already noted, the bound vorticity in the jet sheet in the outer region makes no contribution to the lift. Therefore, the loading along the wing can be simply determined, at least to this order, by the same argument used for the lifting line theory without the jet flap, provided the lift derivative $\partial C_L^{(2)}/\partial \alpha$ is that for jet flapped airfoils of (4.14).

Wing d: rectangular wing

$$\left. \begin{aligned} \frac{C_L}{C_L^{(2)}} &= 1 \left/ \left[1 + \frac{\partial C_L^{(2)}}{\partial \alpha} / 4\pi A \left[\log \left(\frac{8A}{\partial C_L^{(2)}/\partial \alpha} \right) + 1 + \gamma \right] + O\left(\frac{1}{A^2}\right) \right] \right\} \\ \frac{C_{D_i}}{(C_L^{(2)})^2} &= \frac{1}{4\pi A} \left(\log \left(\frac{8A}{\partial C_L^{(2)}/\partial \alpha} \right) + \gamma \right) + O\left(\frac{1}{A^2}\right), \end{aligned} \right\} \quad (6.6)$$

where γ is Euler's constant 0.5772. We note the logarithmic dependence of the aspect ratio A which is distinct from other wing forms. The second term of C_{D_i} has not been determined.

7. Results and discussions

Kerney (1967) and Maskell & Spence (1959) considered only the elliptic case and the following results are given:

Kerney:
$$\frac{C_L}{C_L^{(2)}} = 1 \left/ \left[1 + \frac{1}{\pi A} \frac{\partial C_L^{(2)}}{\partial \alpha} - 2 \frac{C_j}{\pi A} \right] \right. \quad (7.1)$$

Maskell & Spence:

$$\frac{C_L}{C_L^{(2)}} = [1 + (2C_j/\pi A)] \left/ \left[1 + \frac{1}{\pi A} \frac{\partial C_L^{(2)}}{\partial \alpha} + \frac{1}{\pi A} \left\{ \frac{\partial C_L^{(2)}}{\partial \alpha} - 2\pi - 2\pi\sigma \right\} \right] \right. \quad (7.2)$$

Kerney has ignored the circulation in the outer jet sheet. With this effect taken into account, (7.1) reduces to the present result (6.4). Maskell & Spence introduced σ in (7.2) as a small positive quantity describing the deviation of $\alpha_{i\infty}$ from the conventional value $2\alpha_i$

$$\sigma = 1 - \frac{2\alpha_i}{\alpha_{i\infty}}$$

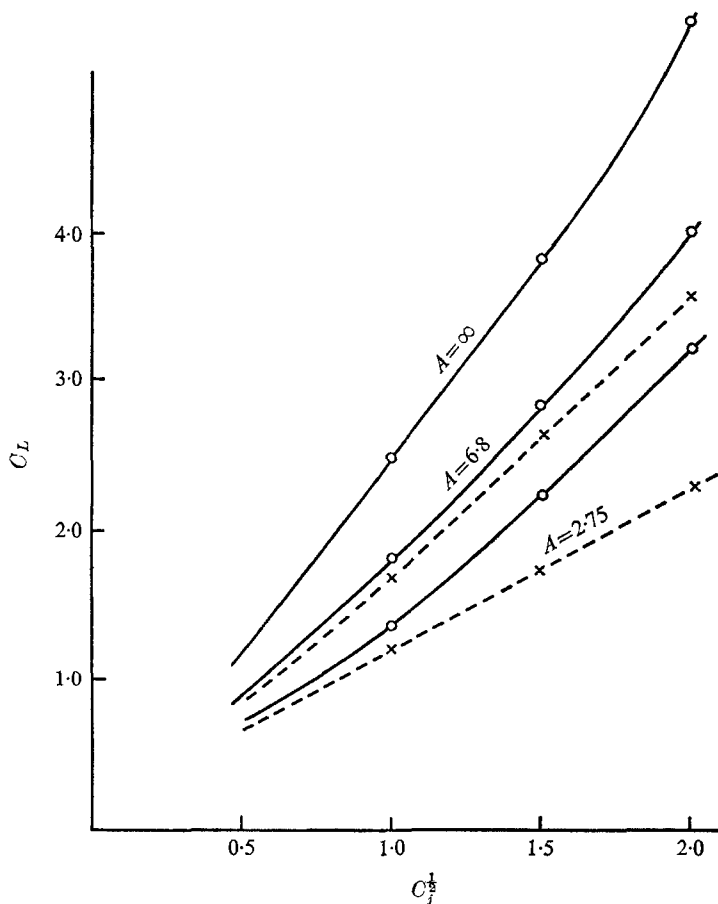


FIGURE 3. Lift curve for three-dimensional jet-flapped wing. Rectangular wing; $\tau = 31.3^\circ$ and $\alpha = 0$. $\circ\circ$, experiment, Williams & Alexander (1957); —, present theory, rectangular wing; $\times-\times$, corrected. Maskell & Spence (1959), and Kerney (1967), elliptic wing.

The present analysis has established that to $O(A^{-1})$, $\sigma = 0$. But such non-zero value of σ may appear at $O(A^{-2})$ as seen from (4.43) and (4.44). Hence the effect of σ is $O(A^{-2})$. Now their result is consistent with the present result if

$$\partial C_L^{(2)} / \partial \alpha - 2\pi = 2C_j.$$

That this relation holds quite accurately over a wide range of C_j can be seen from figure 4 of their own paper. We see that Maskell & Spence give a correct result but it must be written in the present form (6.4) to be consistent with

asymptotic expressions. If the present formulae for elliptic wings are used with appropriate correction for the thickness effect (Maskell & Spence 1959), it underestimates considerably the experimental data of Williams & Alexander (1957) who used a rectangular wing in their experiments as shown in figure 3. On the other hand, the present result using the formula for a rectangular wing shows remarkable agreement with the experiments for a wide range of C_j , A and also α (see also figure 4). The reason for the disagreement of C_L between the elliptic and rectangular wings becomes clear if we compare the loading distribution along the wing.

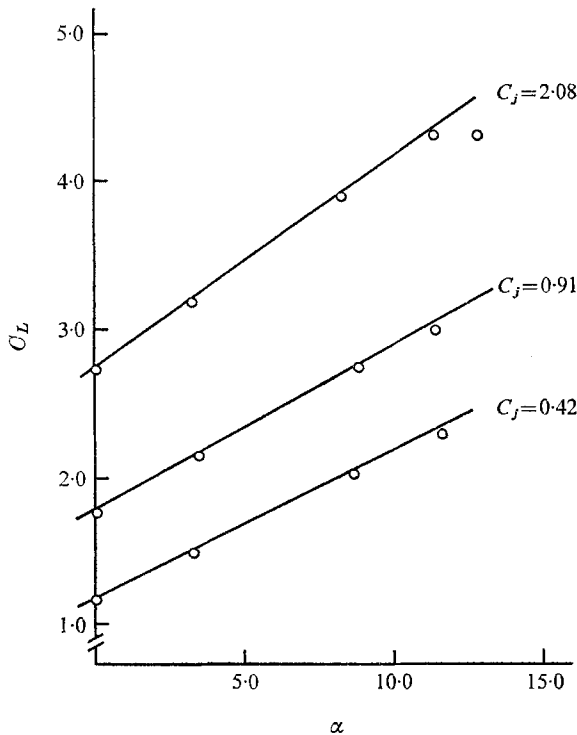


FIGURE 4. Variation of C_L with α and C_j . Rectangular wing; $\tau = 31.3^\circ$ and $A = 6.8$. $\circ\circ$, experiment, Williams & Alexander (1957); —, present theory, rectangular wing.

The load distribution L for elliptic wings is elliptic. Hence

$$L(y)/L^{(2)} = (1-y^2)^{\frac{1}{2}} \left/ \left[1 + \frac{1}{\pi A} \frac{\partial C_L^{(2)}}{\partial \alpha} \right] \right. \quad (7.3)$$

Here $L^{(2)}$ is the load for two-dimensional flow as $A \rightarrow \infty$.

The load distribution for rectangular wings can be computed asymptotically from Stewartson's (1960) solution as

$$L(y)/L^{(2)} = 1 - \frac{1}{1+f(r)} [f(x) + f(r-x)] + O\left(\frac{1}{r^2}\right). \quad (7.4)$$

The function f is the loading function and is tabulated numerically by Stewartson where in our notations

$$r = \frac{8A}{\partial C_L^{(2)}/\partial \alpha} = \frac{4Ae}{\pi}, \quad x = \frac{4A}{\partial C_L^{(2)}/\partial \alpha} (1-y) = \frac{2Ae}{\pi} (1-y). \quad (7.5)$$

We have introduced the effective aspect ratio Ae for the jet-flapped wing

$$Ae = A \frac{2\pi}{\partial C_L^{(2)}/\partial \alpha}. \quad (7.6)$$

We see that, with the use of the effective aspect ratio Ae , all the expressions for C_L given in §6 will reduce to those without the flap. We confirm that as C_L increases, $\partial C_L^{(2)}/\partial \alpha$ increases thus Ae is reduced.

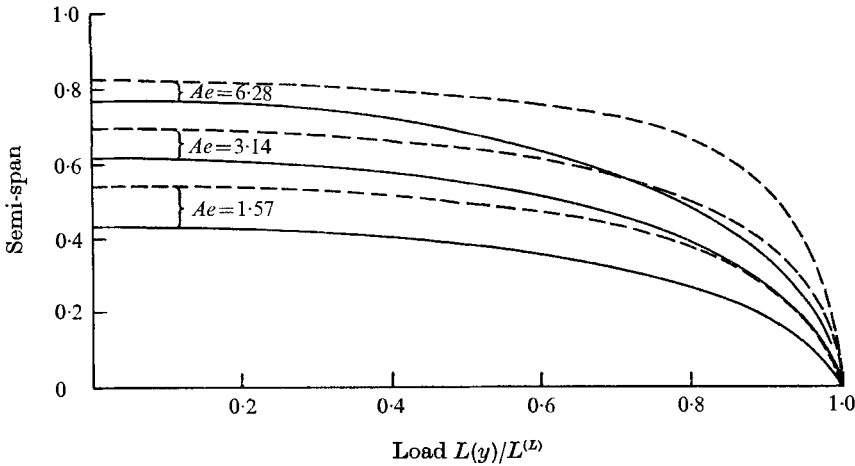


FIGURE 5. Load distribution for elliptic and rectangular wings. - - -, rectangular wings; —, elliptic wing. $Ae = A \times 2\pi/(\partial C_L^{(2)}/\partial \alpha)$.

The load distribution for several values of Ae is plotted in figure 5 using (7.3) and (7.4). Considerable differences exist between the loading of the two wings which clearly account for the disagreement in C_L . It is noted that, except for high aspect ratios, the load distribution for rectangular wings is very close to being elliptic, although the scale of $L(y)$ differs from that of corresponding elliptic wings. See also the measurement of the load distribution by Das (1965) which supports this. This point is further confirmed by the plot of the drag-lift ratio in figure 6. At $A = 6.8$ which corresponds to $Ae \approx 3.5 \sim 4.5$ since $\partial C_L^{(2)}/\partial \alpha \approx 10 \sim 12$ this ratio C_{D_i}/C_L differs very little for rectangular and elliptic wings which must be the minimum as is well known. As expected, this ratio starts to increase considerably for parabolic and cusped wings.

Stimulating discussions on the subject with Professor M. J. Lighthill have been most useful. The present work was completed at the Department of Applied Mathematics and Theoretical Physics, the University of Cambridge, while the author was a visitor. The author wishes to express his deep appreciation to Professor G. K. Batchelor for the hospitality during his stay. The present work was conducted for Lockheed Georgia Company.

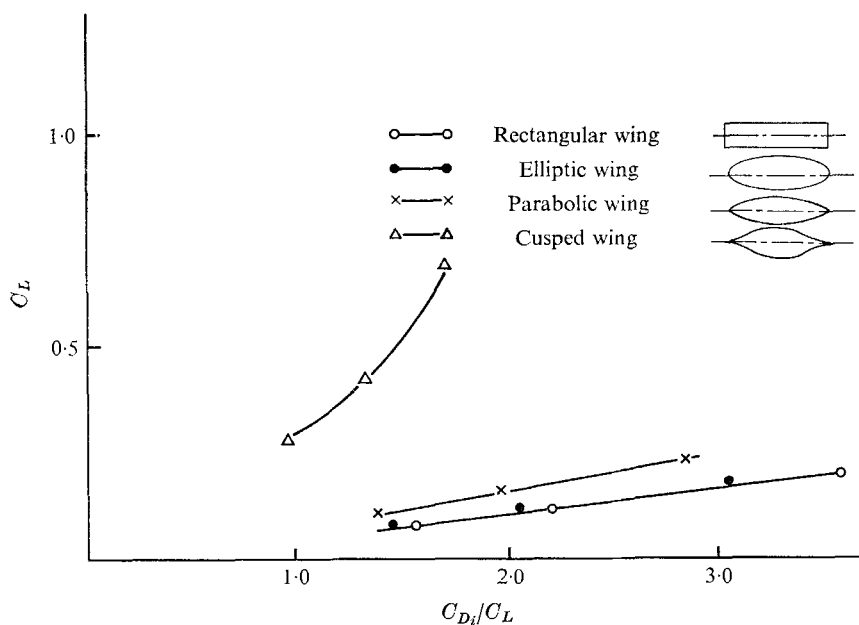


FIGURE 6. Variation of C_{Di}/C_L for various wings; $\tau = 30^\circ$, $\alpha = 0^\circ$, $A = 6.8$, $C_j = 1 \sim 4$.

Appendix

The integrals necessary in evaluating the induced downwash α_{i_2} , $\alpha_{i_{30}}$, α_{i_3} associated for various wing planforms of (6.1) can be found in the table given by Van Dyke (1956). For constant $C_L^{(2)}$, $\partial C_L^{(2)}/\partial\alpha$ and C_j across the span of the wing, α_{i_2} and $\alpha_{i_{30}}$, $\alpha_{i_{32}}$ are given as follows:

	α_{i_2}	$\alpha_{i_{30}}$
Wing a: cusp	$C_L^{(2)} \frac{4}{3\pi} (y^2 - \frac{1}{2})$	$C_L^{(2)} \frac{\partial C_L^{(2)}}{\partial \alpha} \frac{16}{9\pi^2} (-5y^4 + 6y^2 - \frac{9}{8})$
Wing b: lenticular	$C_L^{(2)} \frac{3}{4\pi} \left\{ y \ln \left(\frac{1+y}{1-y} \right) - 2 \right\}$	$C_L^{(2)} \frac{\partial C_L^{(2)}}{\partial \alpha} \frac{9}{32\pi^2} \left[\frac{1}{2}(1-3y^2) \right. \\ \left. \times \left\{ \ln^2 \left(\frac{1+y}{1-y} \right) - \pi^2 \right\} + 6y \ln \left(\frac{1+y}{1-y} \right) \right]$
Wing c: elliptic	$C_L^{(2)} \frac{1}{\pi}$	$C_L^{(2)} \frac{\partial C_L^{(2)}}{\partial \alpha} \frac{1}{\pi^2}$
Wing d: rectangular	$C_L^{(2)} \frac{1}{2\pi(1-y^2)}$	—

$\alpha_{i_{32}}$ can be obtained by merely replacing $\partial C_L^{(2)}/\partial\alpha$ by $-2C_j$ in the expression for $\alpha_{i_{30}}$. With those values of induced downwash, the integration of lift and drag

coefficients are mostly quite straightforward. The only integral not straightforward appears in the integration for wing b of the form

$$\int_{-1}^1 y^4 \ln^2 \left(\frac{1-y}{1+y} \right) dy$$

and this will be obtained below by contour integration.

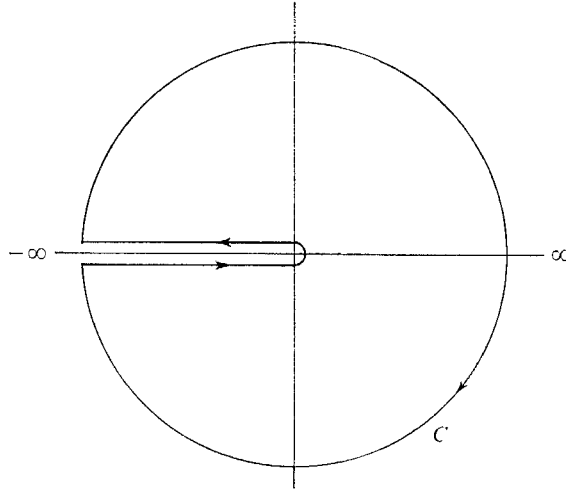


FIGURE 7. Contour C in Z -plane.

Write

$$y = \frac{1-t}{1+t}$$

$$F = \int_{-1}^1 y^4 \ln^2 \frac{1-y}{1+y} dy = 2 \int_0^\infty \frac{(1-t)^4}{(1+t)^6} (\ln t)^2 dt.$$

Consider the following contour integration I

$$I = \int_C f(-z) \{(\ln z)^3 + \pi^2 \ln z\} dz,$$

where

$$f(z) = \frac{(1-z)^4}{(1+z)^6}.$$

We choose contour C around the negative real axis 0 to $-\infty$ and closing it by a large circle as shown in figure 7.

We find

$$I = -6\pi i \int_0^\infty f(t) (\ln t)^2 dt,$$

therefore

$$F = -\frac{2}{3} \text{residue of } I.$$

The residue of the integral I arises from $z = 1$ and is equal to $-(\frac{1}{3}\pi^2 + 4)$. Therefore

$$\int_{-1}^1 y^4 \ln^2 \frac{1-y}{1+y} dy = \frac{2}{3} (\frac{1}{3}\pi^2 + 4).$$

Similarly we find

$$\int_{-1}^1 y^2 \ln^2 \frac{1-y}{1+y} dy = \frac{2}{3}(\frac{1}{3}\pi^2 + 4),$$

$$\int_{-1}^1 \ln^2 \frac{1-y}{1+y} dy = \frac{2}{3}\pi^2.$$

Using this result, the lift and drag coefficients given in (6.2) to (6.4) can be found.

REFERENCES

- ACKERBERG, R. C. 1968 *J. Fluid Mech.* **38**, 261–272.
- ASHLEY, H. & LANDAHL, M. T. 1968 *Aerodynamics of Wings and Bodies*. Addison–Wesley.
- DAS, A. 1965 *Sonderdr. Abhand. Braunsch. Wiss. Gessell.* **17**, 21–48.
- DAVIDSON, I. M. 1956 *J. Roy. Aero. Soc.* **60**, 25–41.
- HOUNGH, G. R. 1959 Cornell University Master of Aeronautical Engineering Thesis.
- KERNEY, K. P. 1967 Ph.D. Thesis, Graduate School of Aeronautical Engineering, Cornell University.
- LAGERSTROM, P. A. 1964 In *Theory of Laminar Flows* (ed. F. K. Moore). Princeton University Press.
- MASKELL, E. C. & SPENCE, D. A. 1959 *Proc. Roy. Soc. A* **251**, 407–425.
- MULTHOFF, H. 1955 *Aero. Res. Counc. R. & M.* no. 2884.
- SPENCE, D. A. 1956 *Proc. Roy. Soc. A* **238**, 46–68.
- SPENCE, D. A. 1958 *Aero. Quest.* **9**, 395–406.
- SPENCE, D. A. 1961 *Proc. Roy. Soc. A* **261**, 97–118.
- STEWARTSON, K. 1960 *Quart. J. Mech. Appl. Math.* **13**, 49–56.
- TREFFTZ, E. 1921 *Z. angew. Math. Mech.* **1**, 206.
- VAN DYKE, M. D. 1956 *NACA Rep.* 1274.
- VAN DYKE, M. D. 1964 *Perturbation Methods in Fluid Mechanics*. New York: Academic Press.
- WILLIAMS, J. & ALEXANDER, A. J. 1957 *Aero. Quart.* **9**, 395–406.
- WHITHAM, G. B. 1952 *Commun. Pure Appl. Math.* **5**, 301–348.